

Real time enhancement of operator's ergonomics in physical human - robot collaboration scenarios using a multi-stereo camera system

Gerasimos Arvanitis*, Nikos Piperigkos†, Christos Anagnostopoulos†, Aris S. Lalos†, Konstantinos Moustakas*

**Department of Electrical and Computer Engineering, University of Patras, Patra, Greece*

†*Industrial Systems Institute, ATHENA Research Center, Patra, Greece*

arvanitis@ece.upatras.gr, piperigkos@ceid.upatras.gr, anagnostopoulos@isi.gr, lalos@isi.gr, moustakas@upatras.gr

Abstract—In collaborative tasks where humans work alongside machines, the robot's movements and behaviour can have a significant impact on the operator's safety, health, and comfort. To address this issue, we present a multi-stereo camera system that continuously monitors the operator's posture while they work with the robot. This system uses a novel distributed fusion approach to assess the operator's posture in real-time and to help avoid uncomfortable or unsafe positions. The system adjusts the robot's movements and informs the operator of any incorrect or potentially harmful postures, reducing the risk of accidents, strain, and musculoskeletal disorders. The analysis is personalized, taking into account the unique anthropometric characteristics of each operator, to ensure optimal ergonomics. The results of our experiments show that the proposed approach leads to improved human body postures and offers a promising solution for enhancing the ergonomics of operators in collaborative tasks.

Index Terms—operator's ergonomics, anthropometrics, human-robot collaboration, multi-stereo camera system.

I. INTRODUCTION

In manufacturing, when operators are physically interacting with a robot, trying to accomplish a collaborative task, their posture is inevitably influenced by the robot's movement and trajectory [1], [2]. Work-related Musculoskeletal Disorders (WMSD) is a major health problem in developed countries [3] and there is a worldwide interest to reduce the conditions and risk factors [4] that may cause this problem [5], decreasing in this way the substantial costs for therapies and negative impacts on the life quality of operators [6]. To overcome this challenging situation, adapted systems are required, able to be adjusted according to the anthropometrics and special characteristics of each operator, improving their physical situation and ergonomics [7]. In literature, there are a lot of works [8] that have used depth sensors (Kinect) or low-cost RGB devices to compute the Rapid Upper Limb Assessment (RULA) [9], [10] score or to detect awkward postures [11]. To achieve this, open-source landmark estimation libraries [12], [13] are used for calculating the body joint angles. Additionally, a lot of research has been done to improve physical ergonomics [14] in human-robot collaboration [15], [16] by generating task assignments [17], [18], finding the optimal trade-off motions [19], providing wearable feedback [20], estimating

the physical load required in a daily job [21], or providing an automatic assessment of ergonomics [22].

In this study, we operate under the premise that collaborative tasks between robots and humans in industrial environments are typically comprised of pre-defined and known actions for the sake of safety. One factor that can impact the robot's movement is the operator's body characteristics, such as height. This factor does not alter the primary action of the robot (e.g., delivering a tool), but can be utilized to select the optimal adjustment of the robot's position and configuration for optimized ergonomics assessment of the operator (e.g., placing the tool in a comfortable location without causing strain). This adjustment takes place only at the start of the robot's operation, as dynamic adjustments are deemed inappropriate for safety reasons. The adaptation of the robot's trajectory facilitates the improvement of the operator's ergonomics and it is performed based on their unique anthropometric characteristics. The key contributions of this work can be summarized as follows:

- A graph Laplacian-based scheme that provides a 3D landmark optimization, allowing for the best use of available captured information at any time, regardless of the camera source.
- The development of a manufacturing simulator from scratch, emulating robotic movements and operator's actions in human-robot collaboration scenarios.
- A framework that increases the operators' situational awareness regarding uncomfortable work postures that may be harmful in long-term exposure. This is achieved through a personalized anthropometric estimation component that provides a comprehensive ergonomic analysis of the operators' actions during their collaboration with the robot.
- An offline tool, suitable for the ergonomics experts to analyse and evaluate the operator's action and help them to set personalized rehabilitation strategies or recommendations to avoid muscle injuries.

The rest of this paper is organized as follows: In Section 2, we discuss in detail each step of the proposed method. Section 3 presents the experimental results and in Section 4 we draw the conclusions.

II. GENERAL ARCHITECTURE & METHODOLOGY

The architecture of the proposed multi-stereo camera system is illustrated in Fig. 1. In our implementation, the system consists of three stereo cameras placed in strategic locations to provide continuous monitoring of the operator's pose from multiple angles, increasing the possibility of continuously having a good capture of the operator's pose (i.e., a view in front of the operator), at least from one of the cameras, while he/she is freely moving in different directions. We use each RGB

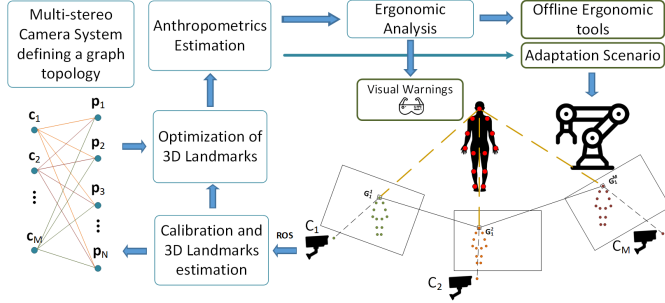


Fig. 1. Proposed concept architecture.

camera of each stereo set to capture the operator's actions. To extract 2D posture landmarks, we utilize the MediaPipe framework [23], which runs locally on the Jetson device where the stereo camera is connected. The extracted landmarks are then sent to a PC server for 3D landmark estimation using a Direct Linear Transform (DLT) triangulation approach [24] and optimization. Next, we estimate the operator's height and calculate their current physical ergonomic state based on the RULA score¹. For seamless integration of the system components and algorithms, we utilize the Robotic Operating System (ROS) as our middleware. The system runs on isolated nodes that communicate using a publish-subscribe model, and we have developed a ROS node for each camera. Each node captures a frame of the camera at a frequency of 10Hz, extracts and processes the landmarks, and publishes them to a relevant ROS topic. The decentralized approach of ROS allows us to connect the cameras to different physical machines, such as the Jetson TX2 embedded device, and all components must be connected to the same local network.

Algorithm 1 summarizes the main steps of the proposed framework. More details will be presented in the next sections.

A. 3D Landmarks Calculation

1) **Single Camera Calibration.** To calibrate each camera individually, we begin by using the same checkerboard pattern positioned in a location that is visible to all cameras at the same time. This step is crucial for performing stereo calibration later. We also ensure that all the used cameras have the same resolution analysis and capture images at the same frame-per-second (fps) ratio to ensure that all captured frames are synchronized [25].

¹<https://ergo-plus.com/rula-assessment-tool-guide>

Algorithm 1: Algorithmic steps of the framework

```

/* A) Calibration steps (It is performed only once) */
1 for i = 1 : M do
2   | Single camera Ci calibration;
3 end
4 for j = 1 : L do
5   | Stereo camera Sj calibration;
6 end
Data: Frames' sequency from the M cameras
Result: Improve operators' physical ergonomics
/* B) 3D landmarks estimation */
7 for i = 1 : M do
8   | /* It runs locally to the Jetson devices */
9   | 2D pose landmark estimation from Ci;
10 end
11 Send the 2D pose landmarks to the central server via ROS;
12 for j = 1 : L do
13   | 3D pose landmark estimation from Sj via DLT
14 end
/* C) 3D landmarks optimization */
15 Follow the steps 1-5 of section II.B;
/* D) Anthropometric and ergonomic analysis */
16 Operator's height estimation;
17 Real-time RULA score analysis;

```

2) **Stereo Calibration.** Let's assume that each camera of the integrated system can be defined as C_i ($\forall i = 1, \dots, 6$) with $\mathbf{c}_i \in \mathbb{R}^{3 \times 1}$ 3D coordinates. The single-camera calibration of camera C_i returns the rotation matrix $\mathbf{R}_i \in \mathbb{R}^{3 \times 3}$, the translation $\mathbf{T}_i \in \mathbb{R}^{3 \times 1}$ matrix and the distortion coefficients. However, the \mathbf{R} and \mathbf{T} matrices alone are not enough to triangulate the 3D points. For the stereo-calibration procedure, we need two sets of cameras. For the sake of simplicity, let's define these two cameras as C_1 and C_2 . Notice here that the same approach can be used for the stereo calibration of all other cameras. The rotation matrix \mathbf{R} and translation vector \mathbf{T} shows how to go from the C_2 coordinate system to the C_1 . We also obtain world coordinates to C_2 rotation and translation, by calculating: $\mathbf{R}_2 = \mathbf{R}\mathbf{R}_1$, $\mathbf{T}_2 = \mathbf{R}\mathbf{T}_1 + \mathbf{T}$. Next, we choose the C_1 position as world space origin ($x = 0, y = 0, z = 0$). Thus, the world origin to C_1 rotation is equal to the identity matrix and translation is a zeros vector. Then, the \mathbf{R} matrix and the \mathbf{T} vector that have been estimated from the previous stereo-calibration step becomes the rotation and translation from world origin to C_2 . Basically, this means that the 3D triangulated points will be in a space with respect to the coordinate system of C_1 's lens. In other words, we simply overlap world coordinates with the coordinates of the C_1 camera. This means $\mathbf{R}_1 = \text{eye}(3)$, $\mathbf{T}_1 = \text{zeros}(3)$ and $\mathbf{R}_2 = \mathbf{R}$, $\mathbf{T}_2 = \mathbf{T}$. Therefore, all triangulated 3D points are measured



Fig. 2. Examples of the simulator in different configurations (height of the operator), corresponding to 3 different anthropometric classes.

from the C_1 camera position in the world.

3) **Direct Linear Transform.** We assume the existence of a 3D point \mathbf{p} in real space with coordinates given as $\mathbf{p} = [x, y, z]$. This point can be observed from both 2 cameras, which have pixel coordinates $\mathbf{G}_i = [u_i, v_i, 1]$ for $C_i, \forall i = 1, 2$. Using the camera projection matrix $\mathbf{K}_i = [\mathbf{R}_i \mathbf{T}_i] \in \mathbb{R}^{3 \times 4}$, \mathbf{G}_i can be written as: $\mathbf{G}_i = \alpha \mathbf{K}_i \mathbf{p}$. In a triangulation problem, we do not know the coordinates of \mathbf{p} . But we can determine the pixel coordinates and the projection matrix through camera calibration. Since \mathbf{G}_i and $\mathbf{K}_i \mathbf{p}$ are parallel vectors, the cross product of these should be zero. The j row vector of \mathbf{K}_i can be written as $\mathbf{k}_j, \forall j = 1, \dots, 4$. This gives us:

$$\begin{bmatrix} u_1 \\ v_1 \\ 1 \end{bmatrix} \times \begin{bmatrix} \mathbf{k}_1 \mathbf{p} \\ \mathbf{k}_2 \mathbf{p} \\ \mathbf{k}_3 \mathbf{p} \end{bmatrix} = \begin{bmatrix} v_1 \mathbf{k}_3 \mathbf{p} - \mathbf{k}_2 \mathbf{p} \\ \mathbf{k}_3 \mathbf{p} - u_1 \mathbf{k}_3 \mathbf{p} \\ u_1 \mathbf{k}_2 \mathbf{p} - v_1 \mathbf{k}_1 \mathbf{p} \end{bmatrix} = \begin{bmatrix} 0 \\ 0 \\ 0 \end{bmatrix} \quad (1)$$

$$\begin{bmatrix} v_1 \mathbf{k}_3 - \mathbf{k}_2 \\ \mathbf{k}_3 - u_1 \mathbf{k}_3 \\ u_1 \mathbf{k}_2 - v_1 \mathbf{k}_1 \end{bmatrix} \mathbf{p} = \begin{bmatrix} 0 \\ 0 \\ 0 \end{bmatrix}$$

This gives us an equation of the form $\mathbf{A}\mathbf{x} = 0$. But the third row is a linear combination of the first two rows giving 2 systems of equations, which is not enough to solve the 3 unknowns in \mathbf{p} . Since we have two cameras, we can extend the matrix to have more rows. In fact, we simply add on more rows for any number of views. This gives us the equation:

$$\begin{bmatrix} v_1 \mathbf{k}_3 - \mathbf{k}_2 \\ \mathbf{k}_3 - u_1 \mathbf{k}_3 \\ u_1 \mathbf{k}_2 - v_1 \mathbf{k}_1 \\ v_2 \mathbf{k}_3 - \mathbf{k}_2 \\ \mathbf{k}_3 - u_2 \mathbf{k}_3 \\ u_2 \mathbf{k}_2 - v_2 \mathbf{k}_1 \end{bmatrix} \mathbf{p} = 0 \quad (2)$$

DLT is a method for calculating a matrix equation of the form $\mathbf{A}\mathbf{p} = 0$. In the real world, there can be some noise, so we write the equation as $\mathbf{A}\mathbf{p} = \mathbf{n}$, and we solve for \mathbf{p} such that \mathbf{n} is minimized. The first step is to determine the SVD decomposition of \mathbf{A} .

$$\mathbf{A}\mathbf{p} = \mathbf{U}\mathbf{S}\mathbf{V}^T \mathbf{p} \quad (3)$$

Our goal is to minimize \mathbf{n} for some \mathbf{p} . This can be done by taking the dot product:

$$\mathbf{n}^T \mathbf{n} = (\mathbf{p}^T \mathbf{V} \mathbf{S} \mathbf{U}^T) \cdot (\mathbf{U} \mathbf{S} \mathbf{V}^T \mathbf{p}) = \mathbf{p}^T \mathbf{V} \mathbf{S}^2 \mathbf{V}^T \mathbf{p} \quad (4)$$

\mathbf{U} and \mathbf{V} are orthonormal matrices and \mathbf{S} is a diagonal matrix. The entries on the diagonal of \mathbf{S} are decreasing, so that the last entry on the diagonal is the minimum value.

Since our goal was to minimize $\mathbf{n}^T \mathbf{n}$, this tells us that it is equivalent to choosing the smallest value of \mathbf{S}^2 by selecting the corresponding column vector of \mathbf{V}^T as \mathbf{p} .

B. 3D Landmark Optimization Algorithm

As a result of varying camera viewpoints and operator movements, we expect that landmarks detected from different cameras will not be the same and may differ in accuracy. Therefore, it is necessary to design a fusion approach that integrates the multi-camera system to provide the best possible landmarks configuration from all the involved cameras. For

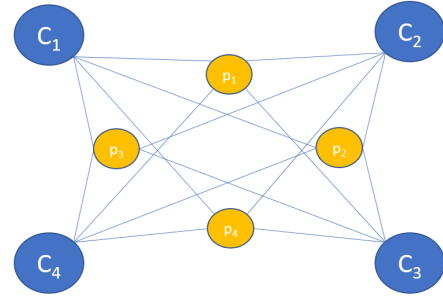


Fig. 3. Indicative example of graph topology for cameras and landmarks.

this task, we create an undirected graph of $N + M$ points $\hat{\mathbf{p}} = [\mathbf{p} \ \mathbf{c}]^T \in \mathbb{R}^{(N+M) \times 3}$, consisting of the N detected landmarks as edges \mathbf{p} , and the M cameras as nodes \mathbf{c} . Fig 3 presents a simplified example of a graph with $M = 4$ and $N = 4$. In order to take advantage of this graph topology formulation, we apply the Graph Laplacian Processing (GLP) technique [26] for re-estimating landmarks in an optimal manner, following the next steps:

1) Encode the spatial relationship of cameras C and landmarks \mathbf{p} via GLP.

2) Construct the binary Laplacian matrix $\mathbf{L} \in \mathbb{R}^{(N+M) \times (N+M)}$ of connectivity graph, indicating which landmark is related to which camera. To mention here that there are not connections between two cameras and between two landmarks.

3) Use as anchor points $\mathbf{a} = [\mathbf{p} \ \mathbf{c}]^T \in \mathbb{R}^{(N+M) \times 3}$ the known location of cameras \mathbf{c} and the average position of landmarks $\bar{\mathbf{p}}^i = \sum_{i=1}^M \mathbf{p}^i \in \mathbb{R}^{N \times 3}$ as estimated by each one of the cameras.

4) Relative measurements and anchors are used to formulate differential coordinates $\delta \in \mathbb{R}^{(N+M) \times 3}$ [27], [28], where the

i^{th} row of δ_i is equal to:

$$\delta_i = [\delta_{xi} \ \delta_{yi} \ \delta_{zi}] = \hat{\mathbf{p}}_i - \frac{1}{|\Psi_i|} \sum_{j \in \Psi_i} \hat{\mathbf{p}}_j = \mathbf{L}\hat{\mathbf{p}}_i, \quad (5)$$

$$\forall i = 1, \dots, N + M$$

where l_i is the i -row of Laplacian matrix, and $|\Psi_i|$ is the number of immediate neighbors of $\hat{\mathbf{p}}_i$.

5) The optimized positions of point $\hat{\mathbf{p}}$ are given by the minimization of the following cost function:

$$\operatorname{argmin}_{\hat{\mathbf{p}}} \left\| \tilde{\mathbf{L}}\hat{\mathbf{p}} - \mathbf{b} \right\|_2^2 \quad (6)$$

where $\tilde{\mathbf{L}} = [\mathbf{L} \ \mathbb{I}_{N+M}]^T \in \mathbb{R}^{2(N+M) \times (N+M)}$, \mathbb{I}_{N+M} is the identity matrix and $\mathbf{b} = [\delta \ \mathbf{a}]^T \in \mathbb{R}^{2(N+M) \times 3}$. Finally, the re-estimated positions of landmarks are derived from linear least-squares minimization:

$$\hat{\mathbf{p}} = (\mathbf{L}^T \mathbf{L})^{-1} \mathbf{L}^T \mathbf{b} \quad (7)$$

To note that during the simulation horizon the topology of landmarks and cameras remains unchanged. As such, the term $(\mathbf{L}^T \mathbf{L})^{-1} \mathbf{L}^T$ is constant and can be computed only once at the start of simulation, in order to be used for the successive frames. In that way, we reduce the computational time required for solving (7) since the costly operation of matrix inversion is performed only at the beginning of the process.

III. EXPERIMENTAL ANALYSIS AND RESULTS

A. Experimental Setup and Implementations

The operating system of the server is UBUNTU 20.04 which is compatible with ROS 1. All the algorithms are written in Python 3.10. There are no special requirements regarding the computational power of the server since the implementation can easily run to low-cost devices (e.g., Jetson).

1) **Operator's Height Estimation.** For this use case two steps are followed: i) Estimation of the operator's height; ii) Adaptation of the robot's position. Once the operator's height has been estimated, the robot's control system receives the information and configures the robot's movement parameters according to the selected scenario. This adaptation ensures that the robot's movements are ergonomically comfortable for the interacting user. 3 different classes c are used, based on the operators' height ($c_1 < 1.68$, $1.68 \leq c_2 \leq 1.82$, $c_3 > 1.82$) (Fig. 2). Each class leads to an adaptable robot response, ensuring that the user can work in an optimal ergonomic state.

2) **Real-Time RULA Estimation.** We perform a real-time joint angle estimation to calculate the RULA score (ranging from 1 to 7, used by ergonomists to evaluate work activities involving upper-body motion [29]). Based on this value, the appropriate warning messages are sent to the operators, informing them if their working pose is ergonomically correct or not (Fig. 4), so as to correct their posture in real-time.

3) **Simulator.** To evaluate the effectiveness of our framework, we have developed an in-house simulation framework from scratch (Fig. 5). The simulator emulates a robotic movement and the corresponding operator's actions in a digital

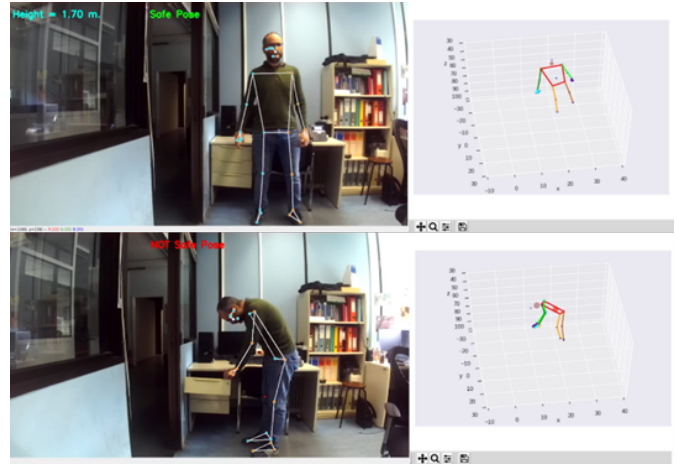


Fig. 4. Safe and wrong pose identification.

workspace created in Unity3D [30]. Fig. 7 presents an example of a user's action before and after the robot's adaptation. 3 stereo cameras are involved, located in 3 different areas of the working environment, monitoring the operator's actions while performs a collaborative tasks with a KUKA robot. The primary objective of the manufacturing simulator is to create a digital twin, which provides a safe environment for evaluating the developed framework and algorithms. Additionally, the simulator can be also used for further ergonomic analysis in order to optimize the workstation of a real industrial environment, so as to obtain a trajectory of the robot as much as possible adapted to the human. Furthermore, the simulator serves as a validation framework since the ground truth information of the 3D landmarks' locations is not known in the real case.

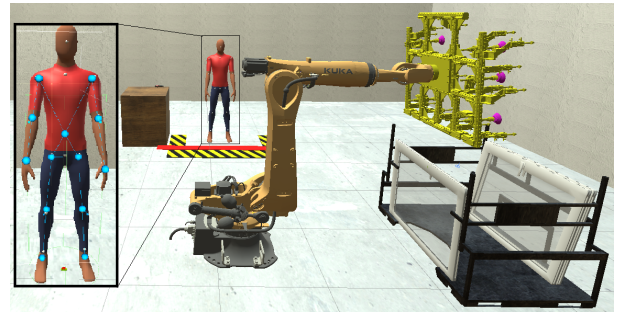


Fig. 5. Screenshot from the environment of the simulator.

4) **Ergonomics Evaluation Tool.** The 3D landmarks are stored and are accessible offline (i.e., 3D view, pause, zoom in/out) by ergonomic experts that can evaluate the poses during a specific action, and suggest how it could be improved. Fig. 6 illustrates an example showing how the joint angles are strained during an action. A heatmap visualizes the level of strength (deep blue is the lowest, deep red is the highest).

B. Experimental Results

Table I summarizes the main outcomes (RMSE values of the 12 landmarks \mathbf{p} , per each stereo camera $S_i \forall i \in (1 - 3)$)

TABLE I
RMSE OF LANDMARKS USING MULTICAMERA SYSTEM AND GLP.

	p_1	p_2	p_3	p_4	p_5	p_6	p_7	p_8	p_9	p_{10}	p_{11}	p_{12}
S_1	0.34	0.38	0.19	0.24	0.15	0.18	0.24	0.27	0.27	0.27	0.22	0.35
S_2	0.36	0.40	0.19	0.28	0.15	0.21	0.27	0.29	0.28	0.32	0.24	0.38
S_3	0.56	0.57	0.34	0.35	0.32	0.30	0.41	0.42	0.43	0.40	0.31	0.43
fusion	0.38	0.39	0.20	0.24	0.16	0.16	0.27	0.27	0.30	0.29	0.21	0.35

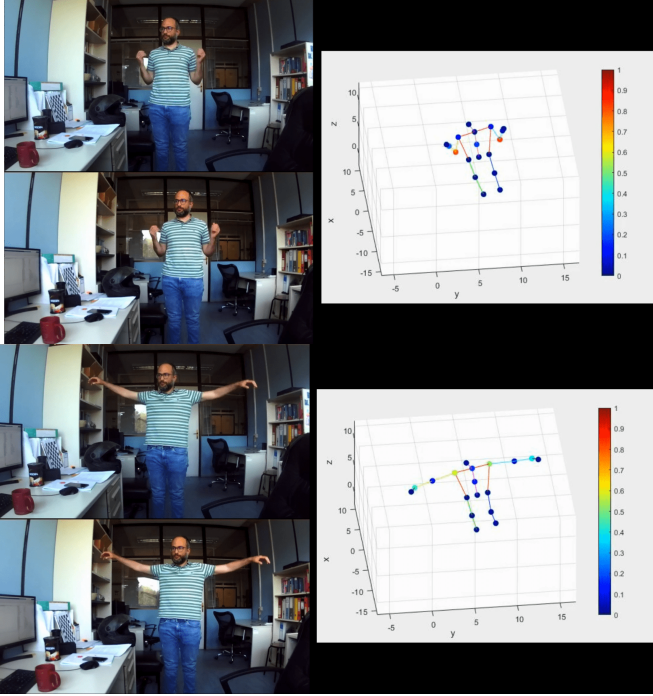


Fig. 6. Ergonomics tool for the evaluation of the joint angles stress.

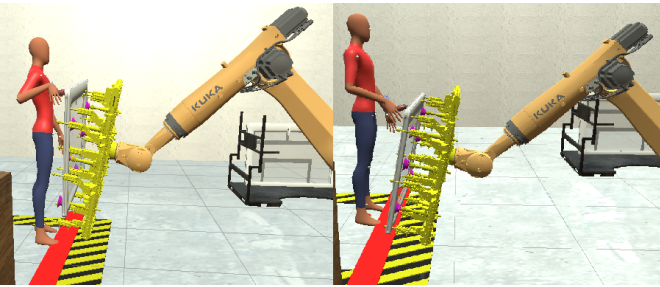


Fig. 7. Screenshot from the environment of the simulator before and after robot's adaptation.

from a testing scenario running in the simulator. As we can see, in most of the cases, the proposed GF-based fusion approach achieved results very close to the optimal, while in two cases (p_6 and p_{11}), landmarks were detected slightly better than the optimal camera. To mention here that the evaluation of the fusion algorithm's performance can be achieved only in a simulated environment since in a real-case scenario the ground truth locations of the landmarks, as well as the accuracy of the cameras, can not be known.

Fig 8 shows a plot with the mean RULA score of different users with different heights (1.5-2 m.) that perform a very

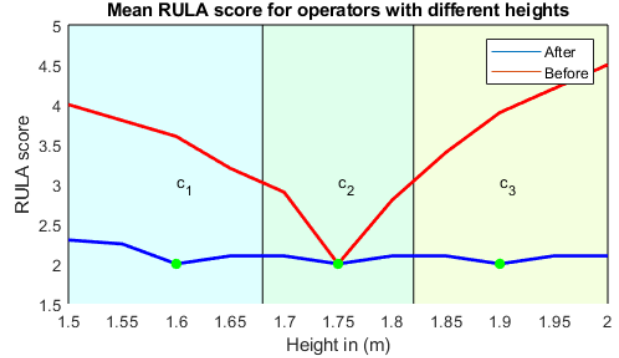


Fig. 8. RULA score for operators with different heights.

specific task before and after the robot's adjustment. As we can see, only operators with 1.75 m. height has a low RULA score before the adaptation, while it is improved for all of the users after the robot's adaptation. Fig 9 shows the mean score per different body areas for all operators. The improvement is more apparent for the cases of "Neck" and "Lower arms". Fig 10 shows how the distribution of the angles per each joint decreases after the robot's adaptation.

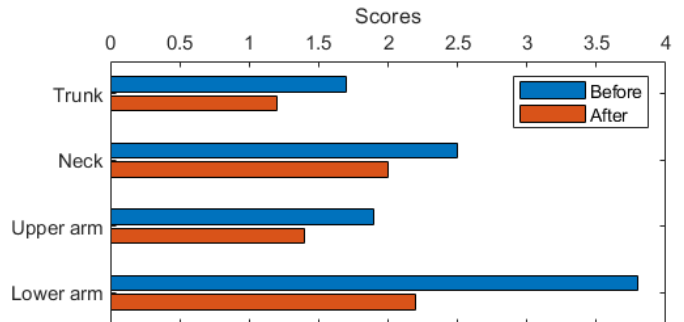


Fig. 9. Mean score per different body areas.

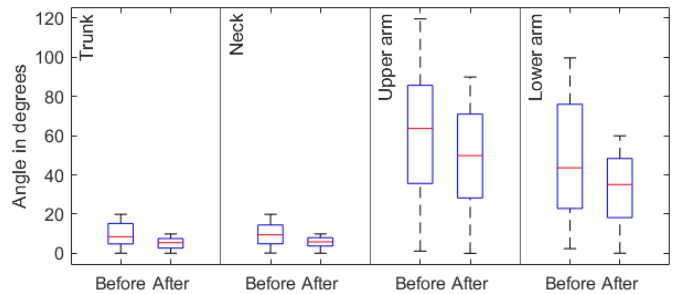


Fig. 10. Distribution of angles per joint.

IV. CONCLUSIONS & FUTURE WORK

In this work, we introduced a multi-stereo camera pipeline aimed at enhancing the operator's physical ergonomics by optimizing the estimation of 3D landmarks. This is achieved in two ways: 1) by adjusting the movement parameters of the collaborative machine to the unique anthropometrics of the operator and 2) by modifying the operator's motion and actions through real-time visual warnings or expert recommendations, based on RULA score estimation. To facilitate the evaluation of our solution, we also developed a simulator. Future plans include implementation in a real industrial setting and a survey to gauge the effectiveness of the method through real user feedback and additionally the evaluation in more complex collaborative tasks.

REFERENCES

- [1] Ilias El Makrini, Kelly Merckaert, Joris De Winter, Dirk Lefeber, and Bram Vanderborght, "Task allocation for improved ergonomics in human-robot collaborative assembly," *Interaction Studies*, vol. 20, no. 1, pp. 102–133, 2019.
- [2] Efstratios Kontopoulos, Gerasimos Arvanitis, Alessandro Zanella, Panagiotis Mitzias, Evangelia I. Zacharaki, Pavlos Kosmides, Nikos Piperigkos, Konstantinos Moustakas, and Aris S. Lalos, "Semantic data integration for monitoring operators' ergonomics in an automotive manufacturing setting," in *The Semantic Web: ESWC 2022 Satellite Events*, Paul Groth, Anisa Rula, Jodi Schneider, Ilaria Tiddi, Elena Simperl, Panos Alexopoulos, Rinke Hoekstra, Mehwish Alam, Anastasia Dimou, and Minna Tamper, Eds., Cham, 2022, pp. 303–306, Springer International Publishing.
- [3] Pauline Maurice, Vincent Padois, Yvan Measson, and Philippe Bidaud, "Human-oriented design of collaborative robots," *International Journal of Industrial Ergonomics*, vol. 57, pp. 88–102, 2017.
- [4] Soheil Gholami, Marta Lorenzini, Elena De Momi, and Arash Ajoudani, "Quantitative physical ergonomics assessment of teleoperation interfaces," *IEEE Transactions on Human-Machine Systems*, vol. 52, no. 2, pp. 169–180, 2022.
- [5] André Cardoso, Ana Colim, Estela Bicho, Ana Cristina Braga, Marino Menozzi, and Pedro Arezes, "Ergonomics and human factors as a requirement to implement safer collaborative robotic workstations: A literature review," *Safety*, vol. 7, no. 4, 2021.
- [6] Marta Lorenzini, Wansoo Kim, Elena De Momi, and Arash Ajoudani, "A new overloading fatigue model for ergonomic risk assessment with application to human-robot collaboration," in *2019 International Conference on Robotics and Automation (ICRA)*, 2019, pp. 1962–1968.
- [7] Sujee Lee, Li Liu, Robert Radwin, and Jingshan Li, "Machine learning in manufacturing ergonomics: Recent advances, challenges, and opportunities," *IEEE Robotics and Automation Letters*, vol. 6, no. 3, pp. 5745–5752, 2021.
- [8] Ernesto Rocha-Ibarra, Marvella-Izamar Oros-Flores, Dora-Luz Almanza-Ojeda, Gabriel-Armando Lugo-Bustillo, Andres Rosales-Castellanos, Mario-Alberto Ibarra-Manzano, and Juan Carlos Gomez, "Kinect validation of ergonomics in human pick and place activities through lateral automatic posture detection," *IEEE Access*, vol. 9, pp. 109067–109079, 2021.
- [9] Pierre Plantard, Hubert P. H. Shum, Anne-Sophie Le Pierres, and F. Multon, "Validation of an ergonomic assessment method using kinect data in real workplace conditions," *Applied ergonomics*, vol. 65, pp. 562–569, 2017.
- [10] Darius Nahavandi and Mohammed Hossny, "Skeleton-free rula ergonomic assessment using kinect sensors," *Int. Dec. Tech.*, vol. 11, no. 3, pp. 275–284, jan 2017.
- [11] Vito Modesto Manghisi, Antonio Emmanuele Uva, Michele Fiorentino, Vitoantonio Bevilacqua, Gianpaolo Francesco Trotta, and Giuseppe Monno, "Real time rula assessment using kinect v2 sensor," *Applied Ergonomics*, vol. 65, pp. 481–491, 2017.
- [12] Z. Cao, G. Hidalgo, T. Simon, S. Wei, and Y. Sheikh, "Openpose: Realtime multi-person 2d pose estimation using part affinity fields," *IEEE Transactions on Pattern Analysis Machine Intelligence*, vol. 43, no. 01, pp. 172–186, jan 2021.
- [13] Woojoo Kim, Jaeho Sung, Daniel Saakes, Chunxi Huang, and Shuping Xiong, "Ergonomic postural assessment using a new open-source human pose estimation technology (openpose)," *International Journal of Industrial Ergonomics*, vol. 84, pp. 103164, 2021.
- [14] Ilias El Makrini, Glenn Mathijssen, Sten Verhaegen, Tom Verstraten, and Bram Vanderborght, "A virtual element-based postural optimization method for improved ergonomics during human-robot collaboration," *IEEE Transactions on Automation Science and Engineering*, vol. 19, no. 3, pp. 1772–1783, 2022.
- [15] Marianna Ciccarelli, Alessandra Papetti, Cecilia Scoccia, Giacomo Menchi, Leonardo Mostarda, Giacomo Palmieri, and Michele Germani, "A system to improve the physical ergonomics in human-robot collaboration," *Procedia Computer Science*, vol. 200, pp. 689–698, 2022, 3rd International Conference on Industry 4.0 and Smart Manufacturing.
- [16] Amir Yazdani, Roya Sabbagh Novin, Andrew Merryweather, and Tucker Hermans, "Ergonomically intelligent physical human-robot interaction: Postural estimation, assessment, and optimization," 2021.
- [17] Margaret Pearce, Bilge Mutlu, Julie Shah, and Robert Radwin, "Optimizing makespan and ergonomics in integrating collaborative robots into manufacturing processes," *IEEE Transactions on Automation Science and Engineering*, vol. 15, no. 4, pp. 1772–1784, 2018.
- [18] Baptiste Busch, Guilherme Maeda, Yoan Mollard, Marie Demangeat, and Manuel Lopes, "Postural optimization for an ergonomic human-robot interaction," in *2017 IEEE/RSJ International Conference on Intelligent Robots and Systems (IROS)*, 2017, pp. 2778–2785.
- [19] Waldez Gomes, Pauline Maurice, Eloïse Dalin, Jean-Baptiste Mouret, and Serena Ivaldi, "Multi-objective trajectory optimization to improve ergonomics in human motion," *IEEE Robotics and Automation Letters*, vol. 7, no. 1, pp. 342–349, 2022.
- [20] Wansoo Kim, Marta Lorenzini, Kağan Kapıcıoğlu, and Arash Ajoudani, "Ergotac: A tactile feedback interface for improving human ergonomics in workplaces," *IEEE Robotics and Automation Letters*, vol. 3, no. 4, pp. 4179–4186, 2018.
- [21] Marta Lorenzini, Wansoo Kim, and Arash Ajoudani, "An online multi-index approach to human ergonomics assessment in the workplace," *IEEE Transactions on Human-Machine Systems*, vol. 52, no. 5, pp. 812–823, 2022.
- [22] Adrien Malaisé, Pauline Maurice, Francis Colas, and Serena Ivaldi, "Activity recognition for ergonomics assessment of industrial tasks with automatic feature selection," *IEEE Robotics and Automation Letters*, vol. 4, no. 2, pp. 1132–1139, 2019.
- [23] Charles Andrew Q. Bugarin, Juan Miguel M. Lopez, Scud Gabriel M. Pineda, Ma. Franziska C. Sambrano, and Pocholo James M. Loresco, "Machine vision-based fall detection system using mediapipe pose with iot monitoring and alarm," in *2022 IEEE 10th Region 10 Humanitarian Technology Conference (R10-HTC)*, 2022, pp. 269–274.
- [24] Y.I Abdel-Aziz, H.M. Karara, and Michael Hauck, "Direct linear transformation from comparator coordinates into object space coordinates in close-range photogrammetry*," *Photogrammetric Engineering and Remote Sensing*, vol. 81, no. 2, pp. 103–107, 2015.
- [25] Vaishnav Chunduru, Mrinalkanti Roy, Dasari Romit N. S, and Rajeevlochana G. Chittawadigi, "Hand tracking in 3d space using mediapipe and pnp method for intuitive control of virtual globe," in *2021 IEEE 9th Region 10 Humanitarian Technology Conference (R10-HTC)*, 2021, pp. 1–6.
- [26] Nikos Piperigkos, Aris S. Lalos, Kostas Berberidis, and Christos Anagnostopoulos, "Cooperative multi-modal localization in connected and autonomous vehicles," in *2020 IEEE 3rd Connected and Automated Vehicles Symposium (CAVS)*, 2020, pp. 1–5.
- [27] Olga Sorkine-Hornung, "Laplacian mesh processing," in *Eurographics*, 2005.
- [28] Gerasimos Arvanitis, Aris S. Lalos, and Konstantinos Moustakas, "Fast spatio-temporal compression of dynamic 3d meshes," in *2021 IEEE 23rd International Workshop on Multimedia Signal Processing (MMSp)*, 2021, pp. 1–6.
- [29] Lynn McAtamney and E. Nigel Corlett, "Rula: a survey method for the investigation of work-related upper limb disorders," *Applied Ergonomics*, vol. 24, no. 2, pp. 91–99, 1993.
- [30] Pavlou M., Laskos D., Zacharaki E., Risvas K., and Moustakas K., "Xrsise: An xr training system for interactive simulation and ergonomics assessment," *Frontiers in Virtual Reality*, vol. 2, pp. 17, 2021.